Polymer Bulletin
https://doi.org/10.1007/s00289-022-04411-y

ORIGINAL PAPER

Amelioration of ionic conductivity (303 K) with the supplement of MnO_2 filler in the chitosan biopolymer electrolyte for magnesium batteries

P. Adlin Helen[1] · P. Christopher Selvin[1] · D. Lakshmi[2] · M. Infanta Diana[1]

Received: 24 April 2022 / Revised: 12 July 2022 / Accepted: 25 July 2022

Abstract

In the present work, the significance of adding MnO_2 filler towards the development of biopolymer electrolyte and chitosan with enhanced ionic conductivity has been reported. The complexation that has been taken place with the inclusion of $MgNO_3.6H_2O$ salt and MnO_2 filler in the chitosan matrix has been investigated through the Fourier transform infrared (FTIR) spectra analysis. Further, the transport parameter values such as number of charge carrier densities (n), mobility (μ) and diffusion coefficient (D) have been calculated from the deconvoluted FTIR spectra. X-Ray diffraction (XRD) and differential scanning calorimetric (DSC) examination revealed that the inclusion of filler significantly reduced the degree of crystallinity and the glass transition T_g values, respectively. These findings show that the inclusion of filler increases the segmental mobility of the polymer chains, allowing for faster ion transport. The conduction properties of the prepared electrolytes have been determined using alternating current (AC) impedance analysis, with the electrolyte containing 60 wt% magnesium salt $(2.6 \pm 0.08) \times 10^{-4}$ S cm^{-1} achieving the maximum ionic conductivity value at room temperature (303 K). This value is further increased by one order of magnitude with the addition of MnO_2 filler into the polymer matrix $(1.25 \pm 0.09) \times 10^{-3}$ S cm^{-1}. To elucidate the individual contributions of ions and electrons in the conduction process, the direct current (DC) polarization method has been used to determine the transference number (t_{ion}) of the produced electrolytes. The filler-added chitosan polymer exhibits an extended electrochemical stability window, 1.7 V, as determined by linear sweep voltammetry (LSV).

Keywords Biopolymer · Magnesium · Battery · Filler · Conductivity · Transference number

✉ P. Christopher Selvin
csphysics@buc.edu.in

Extended author information available on the last page of the article

Published online: 13 August 2022

Introduction

Lithium (Li^+) batteries have been playing a remarkable role in many applications such as energy storage grids, consumer electronic devices, including mobiles, laptops, and portable chargers, and most recently in electric vehicle (EV) transportations particularly due to its outstanding properties of high gravimetric energy density, low reduction potential, longevity and good cyclic stability [1]. This has led to an increase in demand for more lithium sources, whereas some of commercially available Li^+ batteries suffer from poor thermal, chemical and mechanical stability, resulting in safety issues. Few notable factors are dendrite formation, involvement of toxic and unstable chemicals, thermal stability and so on [2]. Considering these drawbacks, researchers around the world are searching arduously on finding suitable alternatives to replace and reduce the requirements for lithium (Li^+). Along with the other post lithium ion research that includes lithium air, lithium sulphur, sodium (Na^+) and multivalent cations such as magnesium (Mg^{2+}), zinc (Zn^{2+}) and calcium (Ca^{2+}) are being explored for their electrochemical properties. Among these, the multivalent cations are preferred very much since they are cost-effective, less reactive in ambient temperature and most importantly available in abundance. Magnesium (Mg^{2+}) being the fifth most available element on earth is believed to be one of the most suitable alternatives to lithium (Li^+). Also, the volumetric density of Mg^{2+} (3833 mAh mL^{-3}) metal is higher than Li^+ (2061 mAh mL^{-3}) metal [3]. The electro-chemistries of magnesium (Mg^{2+}) batteries are similar to Li^+ batteries, but the former suffers from challenges like the lack of good compatible electrolytes with Mg^{2+} metal anode and limited cathode availability with high specific capacity when compared to lithium electrodes [4]. While some liquid electrolytes such as Grignard reagents and tetrahydrofuran (THF) are quite compatible with magnesium metal anode, they undergo sluggish kinetics due to the fact that most of the multivalent cations possess high charge densities and also constitute safety risks similar to organic electrolytes of lithium batteries. On the other hand, utilizing polymer electrolytes are considered to be one of the promising approaches to overcome these challenges as they are known for properties like leakage proof, ease of fabrication, good physicochemical stability, compatibility and good interfacial contact with the electrodes. Polymer electrolytes are comparable to aqueous electrolytes in that they are made up of a polymer matrix that contains a dissociated salt [5].

Numerous works involving the investigations of synthetic polymers like poly (ethylene oxide) (PEO), polyvinylidene difluoride (PVDF), poly (methyl methacrylate) (PMMA) have been reported for various applications including Li^+/Na^+ batteries, supercapacitors, fuel cells, actuators, etc. [6, 7]. It is reported that most of these polymers in general exhibit very poor thermal stability and conductivity at room temperature for magnesium batteries [8]. Many strategies have been reported utilizing filler and other additives such as plasticizers, ionic liquids, blending and copolymerization for enhancing the physical and electrochemical properties of the polymer electrolytes for magnesium batteries [9, 10]. Very recently, Ashih Gupta and his co-workers studied the effect of

1-ethyl-3-methylimidazolium tetrafluoroborate ($EMIMBF_4$) ionic liquid on the structural and electrochemical properties of poly (vinylidene fluoride-hexafluoropropylene) (PVDF-HFP) utilizing Mg (ClO_4) [11]. The addition of ionic liquid depressed the crystallinity in the polymer matrix, thereby enhancing the ionic conductivity up to 8.3×10^{-3} S cm^{-1}. The EDLC properties of biodegradable blended polymer electrolytes based on polyvinyl alcohol (PVA) and polystyrene (PS) with magnesium acetate salt have been investigated by Sravanthi et al. [12] and when fabricated the device achieved highest power density of about 312 W/kg. Nidhi [13] and his team incorporated Al_2O_3 filler in the PVDF polymer matrix with magnesium nitrate salt and the conductivity values were increased by two orders of magnitude to 1.01×10^{-4} S cm^{-1} than the polymer without the filler. Ponraj et al. [14] reported the substantial improvement in the ionic conductivity by two orders of magnitude (10^{-5} to 10^{-3}S/cm) in triblock copolymer poly (vinylidene chloride-*co*-acrylonitrile-*co*-methyl methacrylate) (poly (VdCl-*co*-AN-*co*-MMA)) and improved stability window with the addition of succinonitrile plasticizer. DSC and XRD analysis revealed that adding plasticizer to the polymer matrix reduced the glass transition values and increased the amorphous nature of the polymer matrix.

However, the addition of toxic and flammable plasticizers or ionic liquids again highlights the concerns towards fabricating safe electrolytes for batteries and other applications. On that account, ceramic inert fillers like TiO_2, ZrO_2, Ce_2O_3, ZnO, Er_2O_3, carbon-based materials like graphene oxide and CNTs and active fillers like LLZO, LLTO, etc., are considered to be the most reliable choice to enhance the properties of the polymer electrolytes [15]. In the case of inert fillers in polymer electrolytes, the filler plays no direct part in the ionic conduction process, as the name implies. The improvement in conductivity was found due to interactions of the surface groups of the filler particles with polymer chains and the salt [16]. These fillers have been reported to hinder crystallization kinetics, enabling the enhancement of amorphous nature in the polymer matrix [17]. This in turn results in the increase of the free volume as well as the mobility of the polymer segments near the filler surface. With the addition of filler to the polymer matrix, the hopping mechanism associated with polymer segmental motion is observed to be improved [18].

It is worth noting that the synthetic polymers mentioned above are derived from hazardous petroleum sources and pose a major environmental threat besides being very expensive [19]. In contrast, biopolymer electrolytes are biodegradable, cheap and non-toxic since they are derived from natural sources that include polynucleotides, polypeptides, polysaccharides and other structural macromolecules. Some examples of biopolymers are cellulose, starch, lignin, chitosan, agar–agar, pectin, gellan gum, gelatin, sodium alginate, etc. Chitosan, one of the most abundant biopolymers available, is derived from deacetylation of chitin, a polysaccharide present in the crab shell which is also a biowaste and is being investigated widely for its excellent properties, especially in applications like water purification, drug delivery, biosensors, actuators, supercapacitors, etc. [20, 21], and therefore, it has been chosen as the host matrix in the present work. When inorganic salts of lithium, magnesium, sodium and calcium are dispersed into the matrix, the presence of electrons in the characteristic amine and hydroxyl groups of chitosan facilitates the formation

of bonds with the metal cations and anions of those salts. This is considered to be one of the important prerequisites for a polymer electrolyte to dissociate the salt into ions, which in turn affects the structural, thermal and electrochemical properties of the polymer [22].

Magnesium nitrate hexahydrate ($MgNO_3.6H_2O$) has been selected as the magnesium salt of choice for ionic conduction (Mg^{2+}) and MnO_2 as the inert filler for enhancing the conductivity properties for the preparation of chitosan biopolymer electrolytes in this work. MnO_2, one of the widely used metal oxides with very good physical and chemical properties, has been used in variety of applications such as biosensors, biocatalysts and as electrodes in energy storage devices [23, 24]. Yuhan Li et al. studied the enhanced Li^+ ion transport (1.5 times higher) along with reinforced mechanical strength (2.3 times better tensile strength) upon the addition of filler MnO_2 nanosheet than the pure PEO lithium salt complexes [25]. Similarly, Say Min Tan and his team reported the increment of ionic conductivity (5.79×10^{-3} S/cm) with the addition of MnO_2 in the PMMA-PEO-$LiClO_4$ polymer electrolyte plasticized with ethylene carbonate (EC) [26]. As per the literature survey, no works have been reported on developing magnesium conducting chitosan biopolymer electrolyte incorporating MnO_2 filler. On account of this, the effectiveness of using MnO_2 filler in increasing the conductivity and other properties of magnesium conducting biopolymer electrolytes based on chitosan, prepared with $MgNO_3.6H_2O$ salt, have been investigated and the results are stated.

Experimental

Materials used

Chitosan biopolymer (75% deacetylated chitin) has been procured from LOBA chemicals, glacial acetic acid (99% purity) from HiMedia, magnesium nitrate hexahydrate ($MgNO_3.6H_2O$) from HiMedia and manganese dioxide (MnO_2) from SRL chemicals.

Synthesis procedure

The solid polymer electrolytes are prepared with the appropriate amount of chitosan biopolymer dissolved in 100 ml of 1wt% acetic acid solution with different weight percentages of $MgNO_3.6H_2O$ salt added to it. The polymer–salt solution is allowed to stir till it becomes homogenous, and the desired viscosity is obtained. The resultant viscous solutions are then cast on the petri dishes and are made to dry at room temperature. The salt-added polymer electrolytes are named as CN50, CN60, CN70 and CN80 according to the amount of salts added in weight percentages (50, 60, 70 and 80 wt%). Similar procedure is followed to synthesize polymer electrolytes with MnO_2 filler in various amounts (0.5, 1, 2 and 3 wt%), and the samples are named as such: C0.5Mn, C1Mn, C2Mn and C3Mn.

Characterization methods

The XRD analysis of the prepared polymer electrolyte samples has been carried out with the help of PANalytical X'PERT-PRO diffractometer using CuKα source. The changes in the vibrational peak intensity of the functional groups present in the polymer host on adding the salt and MnO_2 filler have been analysed using FTIR (MIRacle 10-ZnSe) instrument. The glass transition temperature (T_g) has been found using DSC analysis (Netzsch), and the weight loss percentage that occurred while subjecting the samples to various range of temperature in N_2 atmosphere is found using thermogravimetric analysis instrument (EXSTAR/6300). The electrochemical properties like measurement of room-temperature ionic conductivity and voltage stability have been investigated through impedance analysis and linear sweep voltammetry (LSV) analysis (Biologic SP 300 workstation in the frequency range 10 Hz to 1 MHz and in the voltage range (0 to 3 V), respectively. The room-temperature transference numbers (t_{ion}) have been measured using DC polarization method in the symmetric SS/PE/SS (SS-Stainless Steel) electrode configuration with the voltage supply of 1 V.

Results and discussion

Functional group analysis

The evidence of functional groups present in the prepared polymer electrolytes has been confirmed using FTIR analysis. Figure 1 shows the FTIR spectra of $MgNO_3.6H_2O$ salt and MnO_2 filler. Through the changes observed in the vibrational peak intensities and shift in wave numbers from Fig. 2, the formation of complex between the polymer host, salt and the filler has been confirmed. The characteristic vibrational peaks observed around 3360 cm^{-1}, 1550 cm^{-1}, 1360 cm^{-1}, 800 cm^{-1} and 670 cm^{-1} are ascribed to = OH stretching, – O bending, N – O asymmetric stretching(ν_3), NO^{3-} deformation and MgO peaks (metal oxygen), respectively, of $MgNO_3.6H_2O$ salt [27]. Figure 2 displays the FTIR spectra of the pure chitosan and chitosan with different weight percentages of salt. With the addition of salt, the intensity of the characteristic peaks of chitosan seen at 3389 cm^{-1} due to O–H stretching groups is found to be reduced and expanded, indicating improved hydrophobicity of the chosen polymer electrolyte. The vibrational peaks at 2978 cm^{-1} assigned to –CH symmetric and asymmetric vibrations of typical polysaccharide have been disappeared on adding the salt. This disappearance of peaks indicates the dissociation of salt into ions, thereby forming complex with the polymer chains via –H bonding [28]. The further notable peaks at 1558 cm^{-1}, 1651 cm^{-1} and 1072 cm^{-1} correspond to symmetric deformation of NH_3^+ (amine II) groups, O = C –NH stretching (carbonyl amide I) and strong C–O–C vibrations, respectively, of the chitosan biopolymer [29].

The shift in the C–N stretching (amideII) vibrational peaks from 1387 cm^{-1} to 1379 cm^{-1} assures the inter-molecular interaction of the polymer matrix with the anion of the salt. According to Rahman et al., this could be due to the weakening

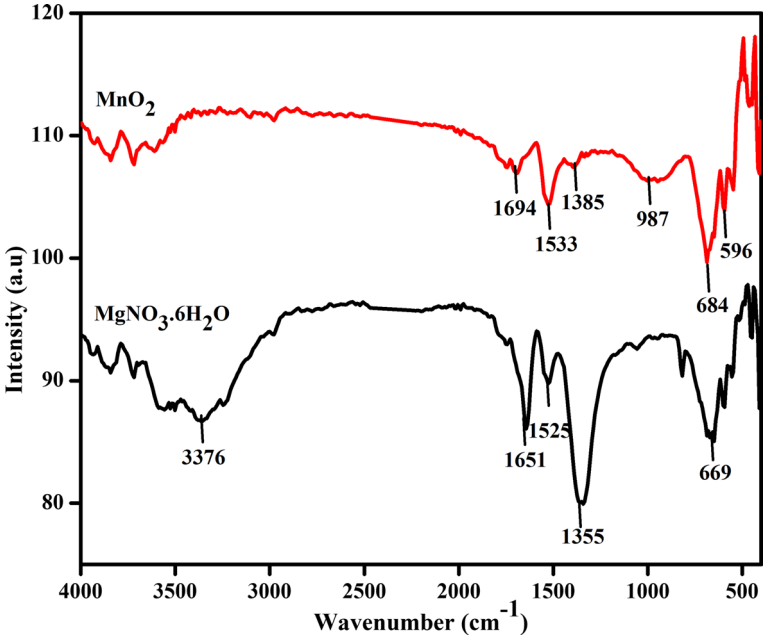

Fig. 1 FTIR spectra of $MgNO_3.6H_2O$ (salt) and MnO_2 (filler)

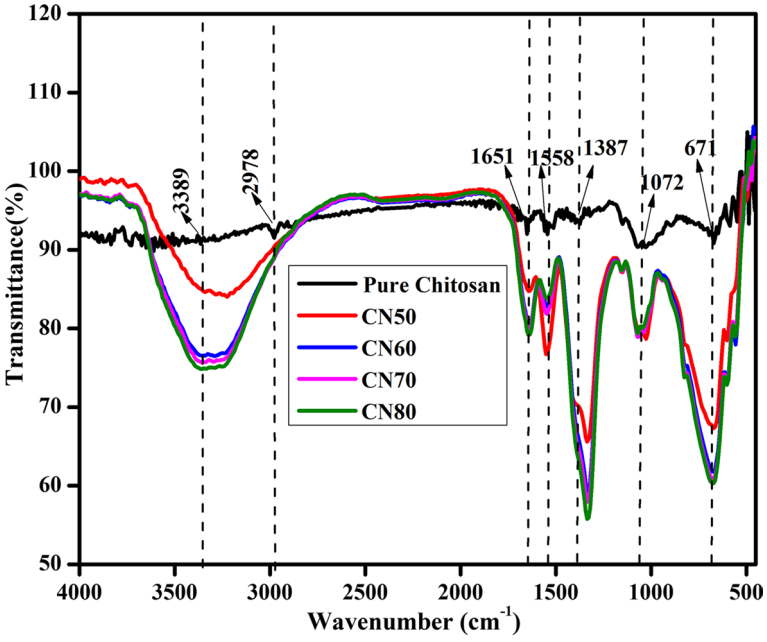

Fig. 2 FTIR spectra of pure chitosan and chitosan with weight percentages of salt

of the interaction or an increase in bond length between the cation and the amine group, both of which would play an important role in ionic mobility when an electric signal is supplied [30]. The changes in intensities found at 671 cm^{-1} indicate the coordinate complex formation between the Mg^{2+} cation with twisting $–NH_2$ vibrational groups with lone pair of electrons (NH_2….Mg^{2+}) [31].

Further from Fig. 1, the vibrational peaks of MnO_2 found at 1694 cm^{-1}, 1533 cm^{-1}, 1385 cm^{-1} and 987 cm^{-1} correspond to –OH bending vibrations complexed with Mn atoms and those around 684 cm^{-1} and 596 cm^{-1} belong to stretching Mn–O bonds present within the MnO_2 structure [32], and the changes observed with the addition of MnO_2 to the polymer electrolyte with 60 wt% salt (CN60) are given in Fig. 3. It should be noticed that while there are no symmetrical changes with the addition of filler, the intensities of the vibrational peaks are much reduced as the filler content is increased. This suggests that the inclusion of filler has a considerable impact on the amorphous nature of polymer electrolytes, which is consistent with the results of the XRD analysis presented in the next section. According to the literature, this is due to the Lewis acid–base like interactions of MnO_2 filler with electron-rich NH_2, oxygen and hydroxyl characteristic groups of the chitosan and also with the ions in the dopant salt in which the cations act as Lewis acid centre and anions as Lewis base centre. These interactions lead to the development of free volume inside the polymer matrix, resulting in a more efficient kinetic pathway for ion migration [33].

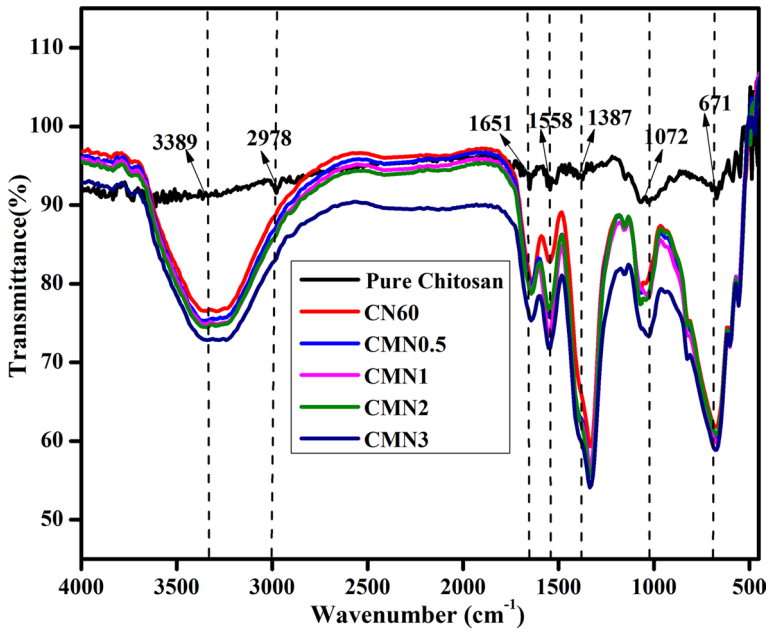

Fig. 3 FTIR spectra of pure chitosan, chitosan with 60wt% of salt and filler in x wt% (0.5, 1, 2, 3)

Analysis of transport parameters from FTIR absorption spectra

The transport properties of ions present in the prepared polymer electrolytes before and after the addition of filler are evaluated by deconvolution of FTIR spectra in absorption mode. The vibrational peak range where changes in peak intensity, shift in wavenumbers observed on adding the salt and then the filler is usually selected for deconvolution and the deconvoluted FTIR responses are presented in Supplementary Information (Fig. S1). Here the deconvolution is carried out for the vibrational peaks in the frequency range between 1500 cm^{-1} and 1200 cm^{-1} belonging to the characteristic peaks of NH_3^+ (amine II) of the polymer (around 1389 cm^{-1}) where a shift to lower wavenumbers due to complexation with anion group (NO_3) in the salt belonging to N–O symmetric stretching vibrations of the ionic salt is observed. The same frequency range is selected for deconvolution of FTIR spectra with MnO_2 filler to compare the calculated values of percentage of free ions. The percentage of free ions and ion aggregates present in the polymer matrix is calculated using Eq. (1):

$$\text{Percentage of free ion (\%)} = \frac{\text{Area of free ions peak}}{\text{Total area (free ions peak + ion pairs peak)}} \times 100\% \quad (1)$$

The calculated values are given in Table 1. It is found that the highest percentage of free ions is found for the electrolyte with 60 wt% of $MgNO_3.6H_2O$ salt (CN60), and this value is reduced with increase in salt concentration above 60wt%. This confirms the formation of ion pairs or ion agglomerates at increasing concentrations of salt. The percentage of free ions in the electrolyte CN60, on the other hand, is observed to be increased when filler is added. This shows that adding the filler causes the salt to dissociate into a greater number of free ions, which could be correlated to the contributory factor in improved ionic conductivity of these polymer electrolytes [34]. Again, this value is decreased on adding MnO_2 filler more than 2 wt%, indicating that the capacity of the polymer matrix

Table 1 Free ion percentage, number of charge carriers (n), mobility (μ) and diffusion coefficient (D) for the prepared polymer electrolytes with variation in salt and filler content

Sample	Free ion (%)	$n(cm^{-3}) \times 10^{22}$	$\mu(cm^2v^{-1}\,s^{-1}) \times 10^{-10}$	$D(cm^2s^{-1}) \times 10^{-11}$
Chitosan + salt				
CN50	40.5	2.3	0.4	1.0
CN60	63.4	5.5	2.9	6.8
CN70	34.4	4.7	1.9	4.4
CN80	11.5	2.5	1.7	4.0
CN60 + MnO_2				
C0.5Mn	64	5.5	0.4	0.8
C1Mn	64.9	5.6	0.3	0.9
C2Mn	70	6.1	1.3	3.0
C3Mn	35.5	3	0.6	1.4

to accommodate the filler particles has reached a threshold, and adding more filler reduces the distance between each ion, resulting in ion agglomeration of filler particles.

To support this further, the transport properties such as ionic mobility (μ), number of charge density (n) and diffusion coefficient (D) values have been calculated using the free ion percentage values employing Eqs. 2, 3 and 4:

$$n = \frac{M \times N_A}{V_{\text{total}}} \times (\text{free ion } \%) \tag{2}$$

$$\mu = \frac{\sigma}{ne} \tag{3}$$

$$D = \frac{\mu kT}{e} \tag{4}$$

where M is the number of moles of salt, N_A is the Avogadro's number, V_{total} is the volume of the polymer electrolytes (cm^3), σ is the ionic conductivity measured from AC impedance analysis (S cm^{-1}), n is the number of charge carriers, e is the electronic charge (1.6×10^{-19} C), k is the Boltzmann constant (1.38×10^{-23} J K^{-1}) and T is the temperature in Kelvin (K) [35]. It is found that the values of these transport parameters obtained as presented in Table 1 are in proportion with the trend observed in the ionic conductivity values (Table 3) obtained for the electrolytes with salt. The values of these transport parameters obtained are increased till 60 wt% of salt in the polymer electrolytes (CN60), after which there is a sudden decline in the values. However, these values are increased with the addition of filler in the CN60 polymer electrolytes. As previously noted in the FTIR spectra analysis, the interaction of filler groups with the ions in the salt results in enhancing the dissociation of salt into a considerable number of free ions, which also leads to creation of free space inside the polymer matrix, allowing the ions to migrate more easily and could be correlated to the increase in the transport parameter values.

Possible conduction mechanism

The probable interaction that could have happened between the salt, filler, and characteristic groups present in the chitosan polymer matrix has been illustrated in Scheme 1 based on the changes found in the vibrational bands from the FTIR analysis (1500 cm^{-1} to 1200 cm^{-1}). The Mg^{2+} cation forms complexes with the electron-rich groups in the polymer backbone, whereas the anion interacts with the carbonyl groups and the amide groups (Scheme 1a). Also the anion radius is bulkier than the radius of cation which hinders its movement inside the polymer matrix and mostly remain immobile than cation during the conduction process [36]. The ion–ion interaction happens when the polymer matrix has exceeded its saturation point for accommodating the ions, resulting in the formation of ion pairs at higher salt concentrations as evident from the calculated free ion values.

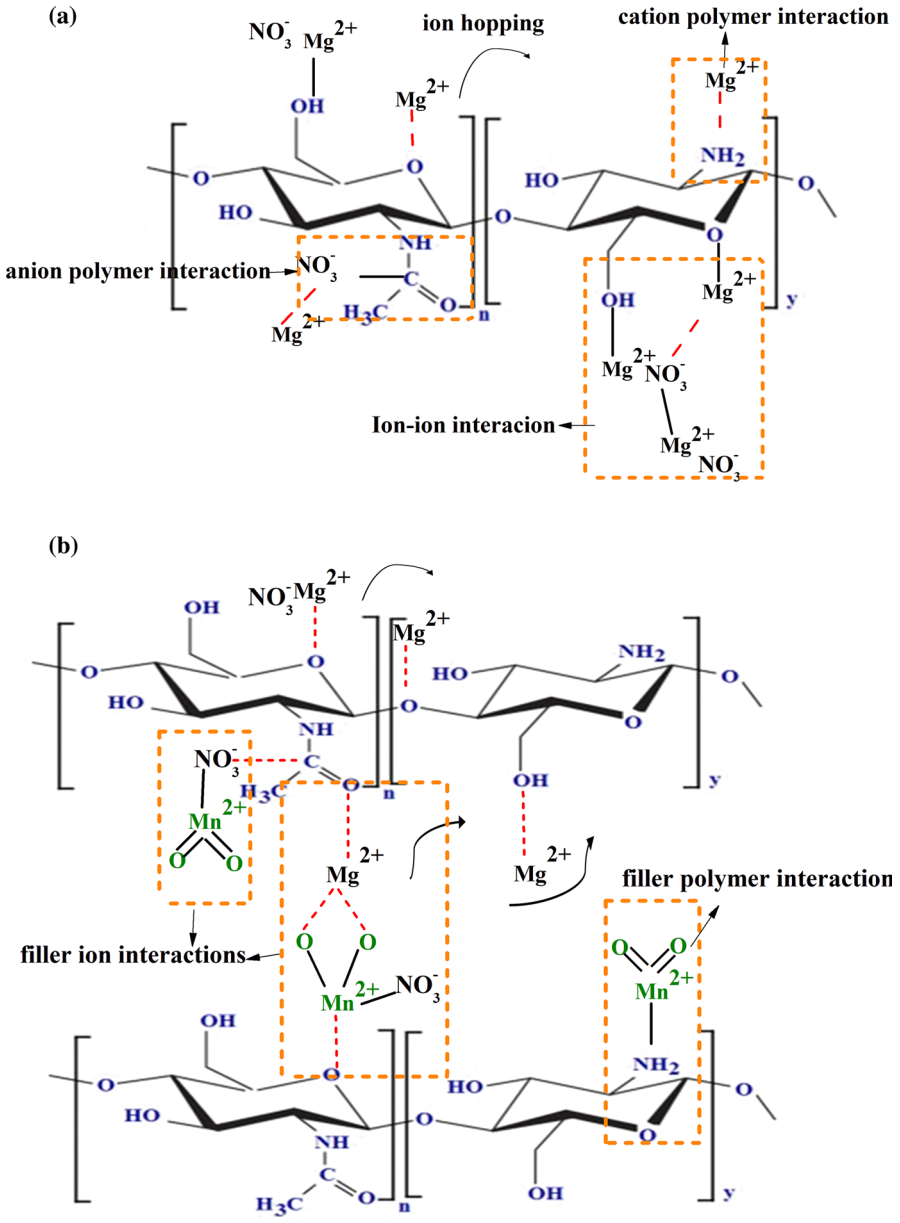

Scheme 1 Possible interaction of polymer with **a** salt and **b** filler groups

On adding MnO_2 filler to the polymer electrolyte CN60 (Scheme 1b), the cations and anions of the salt begin to interact with the surface groups of the MnO_2 filler (filler–ion interaction). Also, the fillers serve as cross-linking centres with the characteristic groups present in the polymer segment (filler–polymer interaction). This is

expected to result in the increase of the free space within the polymer matrix, facilitating the movement of ions from one coordinated site to another.

Structural analysis

Figure 4 shows the XRD diffractograms of the prepared chitosan biopolymer electrolytes with various wt% of $MgNO_3.6H_2O$ salt. The characteristic peaks observed at 15.3° 20° and 30° indicate the semicrystalline nature of the pure chitosan [37]. It should be noted that the addition of salt causes the intensity of the diffracted peaks of the chitosan polymer host to be uplifted. According to Faisal I Chaudry et al. this is due to the interaction of ions in the salt with functional groups existing in the polymer host, such as NH_2 with the lone pair of electrons, as well as other oxygen and hydroxyl groups, and this has been validated by FTIR analysis [38]. However, the intensity is found to be low for the polymer electrolyte with 60 wt% of $MgNO_3.6H_2O$ salt when compared to other salt-added polymer electrolytes and the crystalline nature is found to be increased again at higher concentrations of salt. Also the degrees of crystallinity values are increased initially with the addition of salt. This is in alignment with glass transition values (T_g) obtained from DSC analysis.

It is to be noted that the intensity of the characteristic diffracted peak of CN60 is reduced extensively with the incorporation of MnO_2 filler to the polymer host

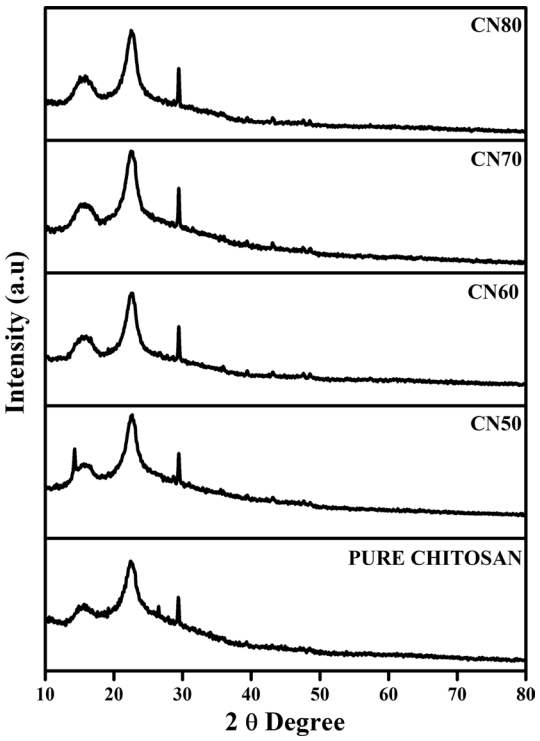

Fig. 4 XRD pattern of pure chitosan and chitosan with different weight percentages of salt

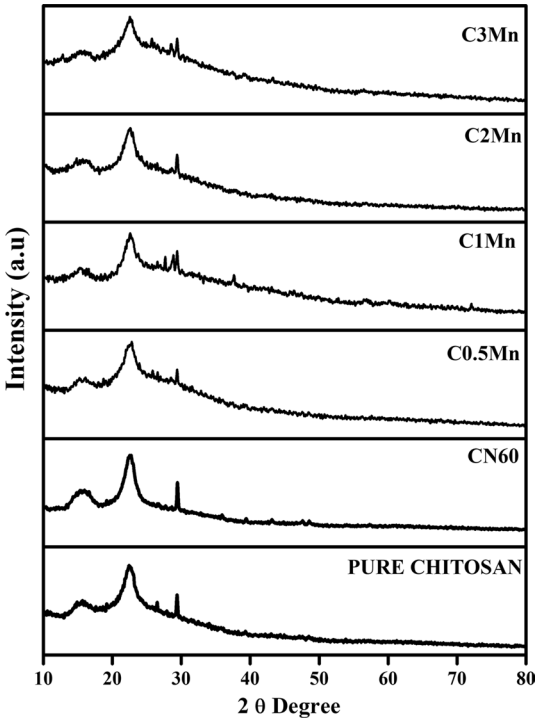

Fig. 5 XRD pattern of pure chitosan, chitosan with 60 wt% of salt (CN60) and CN60 with different weight percentages of filler

Table 2 Degree of crystallinity values calculated for the prepared electrolytes

Sample	Degree of crystallinity (±0.1)
Chitosan + salt	
Pure Chitosan	15.6
CN50	20.5
CN60	16.4
CN70	21.3
CN80	21.8
CN60 + MnO_2	
C0.5Mn	12.1
C1Mn	11.2
C2Mn	8.1
C3Mn	8.9

(CN60) as evident from Fig. 5. Also, this is in agreement with the degree of crystallinity (χ) values obtained using Eq. 5 with the help of area calculated under each crystalline peaks and amorphous peaks in the XRD spectra, and the calculated values are given in Table 2.

$$\chi = \frac{\text{Area of crystalline peaks}}{\text{Total area(Amorphous + Crystalline)}} \times (100\%) \quad (5)$$

This decrease in peak intensity is owing to the addition of filler, which confirms the suppression of recrystallization in the polymer matrix, resulting in an increase in the amorphous phase [39]. This also indicates the increase in free volume inside the host matrix, giving rise to more conduction pathways for free ion mobility. The polymer electrolyte with 2 wt% of filler has shown lowest degree of crystallinity values. However, this value is found to be increased on increasing the filler content above 2 wt%. This rise in crystallinity might be attributed to the creation of ion pairs or ion aggregates inside the polymer matrix, based on the percentage of free ion values determined using deconvolution of FTIR spectra. Furthermore, the absence of any distinct peaks of both salt and filler in the diffractograms obtained for the prepared electrolytes indicates that salt and filler have completely dissociated in the polymer matrix, confirming the interaction that has occurred in the polymer matrix among the characteristic groups with the salt and filler.

DSC and TG analysis

The DSC thermograms exhibiting endothermic peaks for all the prepared polymer electrolytes are given in Fig. 6. The T_g value of pure chitosan is observed to be around 53 °C from Fig. 6 a. This T_g value has been found to be increased initially to 60 °C on adding the salt (Fig. 6b). The ion–dipole interaction between the electron-rich groups in the polymer and the ions in the salt causes the segmental polymer chain dynamics to be reduced, resulting in an increase in T_g value [40]. However, when the salt content is increased to 60%, the T_g value drops, indicating that crystallization is reduced and it confirms the development of transitory cross linkages between the salt and the functional groups present in the polymer matrix, thereby stiffening the polymer. However, as the salt concentration is increased above 60%, the T_g value increases again, which could be due to the agglomeration of ionic clusters of salt groups, which reduces the segmental mobility of the polymer chains. This is also consistent with the crystallinity degree values obtained from XRD diffractograms. It is worth noting that adding MnO_2 filler to polymer CN60 has reduced the glass transition temperature (T_g), indicating the changes happened in the amorphous regions of the prepared polymer electrolytes, making the electrolytes more flexible (Fig. 6c). According to Benson K Money et al. this decrease in T_g after adding the filler confirms the interaction of filler groups with polymer–salt complexes, which accelerates polymer chain dynamics [41]. Increasing the filler content above 2 wt% reduces the T_g value again. The lowest T_g value obtained for polymer with 2 wt% filler is expected to achieve the highest ionic conductivity, which is due to the dipole orientation of filler groups while interacting with polymer functional groups and the salt, resulting in an increase in the amorphous phase inside the matrix, as explained in FTIR analysis. The TG analysis has been performed to examine the reduction in the weight loss percentages of the polymer electrolytes with the addition of filler, as

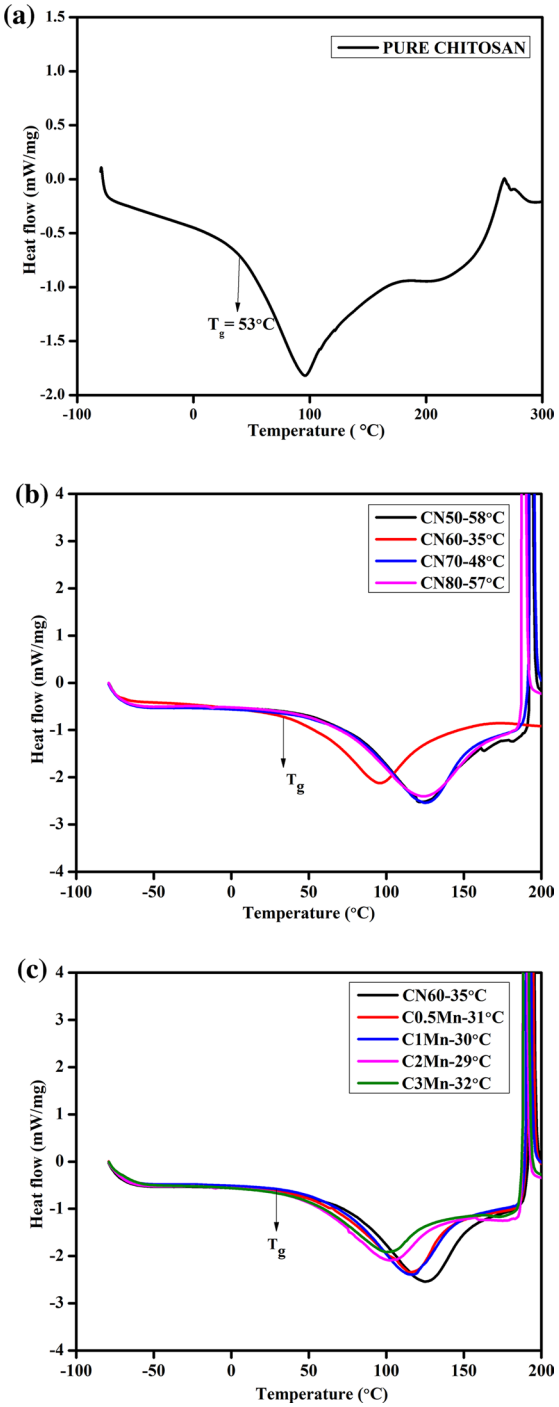

Fig. 6 **a** DSC thermogram of pure chitosan, **b** chitosan with various amounts of salt content **c** chitosan with different amounts of filler

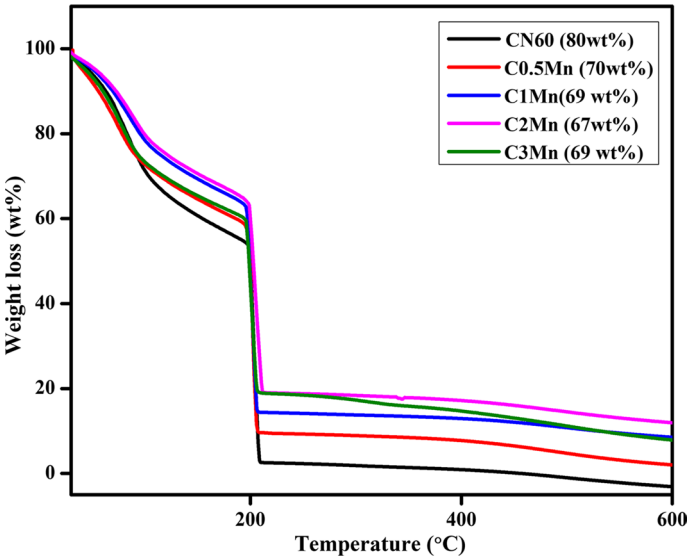

Fig. 7 TG thermograms of CN60 and CN60 with different amounts of filler

shown in Fig. 7. The evaporation of water solvent is primarily accountable for the weight loss observed in all samples at two phases. The inclusion of filler has clearly improved the weight loss percentage to a reasonable proportion, as evidenced by the thermograms. This implies that the filler particles present inside the polymer matrix inhibits the evaporation of solvent and water content in the electrolytes denoting the improvement in the thermal stability [42].

Impedance analysis

The ionic conductivity measurement at room temperature (303 K) has been carried out using impedance analysis, and the Nyquist plots with the corresponding equivalent circuits of the pure chitosan and chitosan with different weight percentages of $MgNO_3.6H_2O$ salt are displayed. For pure chitosan, a depressed semicircle with high bulk resistance (R_b) is obtained (Fig. 8a). However, on adding different weight percentages of salt to the pure chitosan matrix, the value of R_b is decreased as seen from the Nyquist plots (Fig. 8b) exhibiting two depressed semicircles for the salt-added polymer electrolytes. The electrochemical behaviour observed at both the semicircles is represented by the parallel combination of resistance and CPE and the relevant equivalent circuit is given in Fig. 8b. The conductivity values are calculated using Eq. 6,

$$\sigma = \frac{t}{R_b A} \tag{6}$$

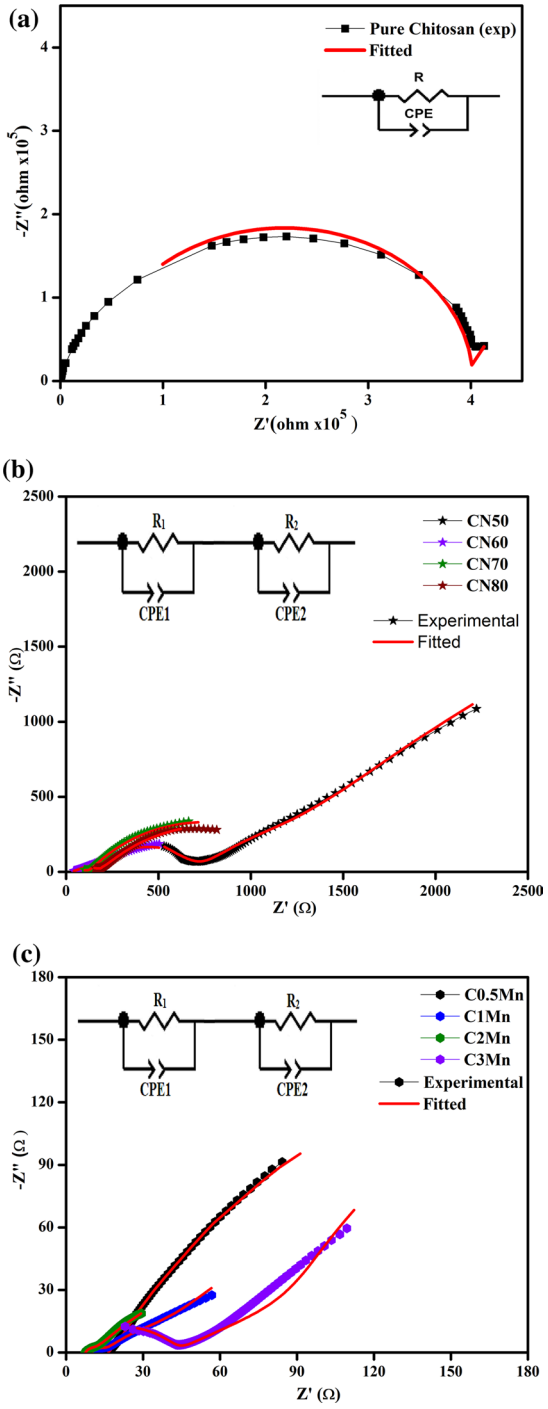

Fig. 8 **a** Nyquists plot of pure chitosan **b** chitosan with salt in different weight percentages **c** chitosan with filler in different filler percentages

where t is the thickness of the electrolytes samples, R_b is the bulk resistance and A is the area of the electrolyte. The first semicircle obtained in the high-frequency region corresponds to parallel combination of bulk resistance (R_b) and the capacitance (non-ideal), whereas the resistance found in the incomplete depressed second semicircle in low-frequency region corresponds to the formation of passive layer resulting from the diffusion of ions at the blocking electrode–electrolyte interface. Therefore, the ionic conductivity of the electrolytes is calculated using the bulk resistance obtained from the first semicircle [43].

A maximum conductivity of about $(2.6 \pm 0.08) \times 10^{-4}$ S cm^{-1} is found in chitosan biopolymer electrolyte with 60 wt% salt (CN60), as expected by DSC and XRD studies. The conductivity values are also found to be declining as the salt concentration is increased over this threshold value of 60 wt%. This decrease in ionic conductivity, according to Koduru et al. is due to the strong columbic attraction that exists between the ions at high salt concentrations, resulting in the creation of ionic salt clusters, as validated by FTIR deconvolution analysis. This in turn hinders the charge carrier transport within the polymer matrix [44]. Figure 8c shows the Nyquist plots of the polymer electrolytes with 60 wt% salt and various amounts of MnO_2 filler (0.5 to 3 wt%). Similar to salt-dispersed chitosan biopolymer electrolytes, two depressed semicircles are observed, whereas the diameter of these semicircles has been reduced extensively that resulted in the augmentation of ionic conductivity values and for the electrolyte with 2 wt% of filler C2Mn achieving the highest value by an increase of one order of magnitude $(1.25 \pm 0.09) \times 10^{-3}$ S cm^{-1}. This is due to the fact that the crystalline phase in the salt-dispersed chitosan polymer matrix is disrupted with the addition of MnO_2 filler, and similar observations have been reported in the literature [45]. This is also in consistent with the decrease in degree of crystallinity and T_g values obtained from XRD and DSC analysis, which further confirms the decrease in the tendency of polymer chains to reorganize due to weakening of coordinative bonds between cations and electron-rich groups in polymer with the addition of filler. Also, the increment in the ionic conductivity values is supported with

Table 3 Conductivity (σ) and Resistance(R) values of the prepared electrolytes

Sample Code	σ (S cm^{-1})
Chitosan + salt (±0.08)	
Pure Chitosan	6.3×10^{-9}
CN50	1.7×10^{-5}
CN60	2.6×10^{-4}
CN70	1.05×10^{-4}
CN80	7.18×10^{-5}
CN60 + MnO_2 (±0.09)	
C0.5Mn	3.33×10^{-4}
C1Mn	3.12×10^{-4}
C2Mn	1.25×10^{-3}
C3Mn	2.84×10^{-4}

the increase in number of charge carrier values and other transport parameters like ionic mobility (μ) and the diffusion coefficient (D) obtained using the free ion percentage values calculated from the deconvolution of FTIR spectra. Due to the influence of local dielectric environment or space charge polarization of the filler, the inclusion of the filler enhances the dissociation of magnesium salts into more number of free charge carriers [46]. The calculated ionic conductivities on adding salt and filler content separately in the polymer electrolyte are given in Table 3, and the corresponding circuit parameter values are presented in Supplementary Information (Table S1). The ionic conductivity values are slightly lower for 1 wt% filler than 0.5 wt% and could be neglected since the values are in same orders of magnitude (Table 3), and the highest value is found at 2 wt% loading of filler in the host matrix.

However, a decline in ionic conductivity value is seen while increasing the filler content above 2 wt%. This implies that the threshold limit of the polymer electrolyte in accommodating filler particles is 2 wt% and that adding more filler particles will only result in the creation of filler clusters, which will prevent charge carriers from moving freely through the interfacial pathway. Many similar works reported related to significant effect in enhancing the ionic conductivity with the addition of fillers in polymer electrolytes are given in Table 4.

Transference number

The transference number (t_{ion}) helps in confirming the ionic contribution of the polymer electrolytes in the conduction process. It is defined as the ratio of current carried by the ions to the total current (I) observed while subjecting the polymer electrolytes to a voltage of 1 V. The steady state achieved after a sudden decline in transient current observed over a period of time (in hours) is given in Figs. 9a and b. The drop in steady-state current (I) shows complete dissociation of ionic species inside the polymer matrix, with the electronic contribution accounting for the remaining current [53].

With the help of the current (I) values obtained at the final and initial stages of polarization, the transference number (t_{ion}) values are calculated employing Eq. 7,

Table 4 List of polymer electrolytes with filler and their conductivities

Polymer	Filler	Ionic salt	Conductivity hike (S cm^{-1})	Reference
PEO	ZrO_2	$NaPF_6$	5×10^{-8} to 3×10^{-6}	47
Corn starch	Al_2O_3	LI	1×10^{-4} to 6×10^{-4}	48
Starch/chitosan	GO	$LiClO_4$	9×10^{-6} to 3×10^{-3}	49
CS/CMC	CNT	$LiClO_4$	1×10^{-4} to 3×10^{-3}	50
Chitosan	ZrO_2	$LiClO_4$	2×10^{-5} to 3×10^{-4}	51
Chitosan	V_2O_5	$MgCl_2$	4×10^{-4} to 1×10^{-3}	52
Chitosan	MnO_2	$MgNO_3.6H_2O$	2×10^{-4} to 1×10^{-3}	Present work

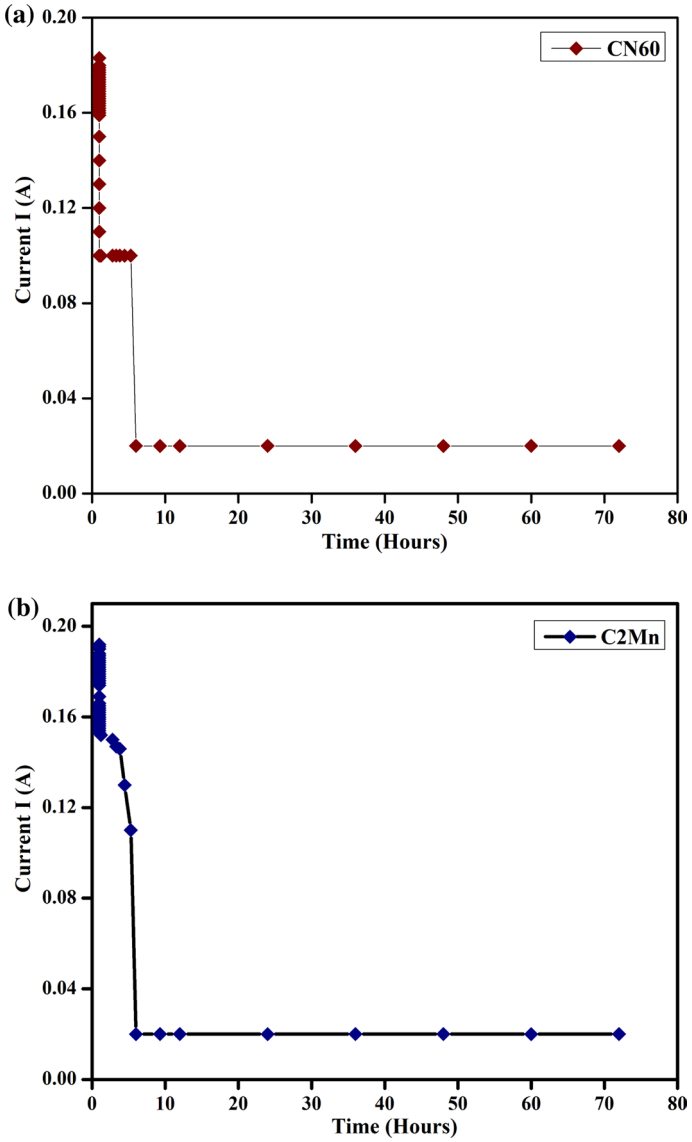

Fig. 9 Transference number measurement of **a** CN60 and **b** C2Mn

$$t_{\text{ion}} = \frac{I_i - I_s}{I_i} \tag{7}$$

where I_i and I_s represent the initial and the steady (final) state current, respectively. The transference number (t_{ion}) is found to be higher close to unity (0.9) for the polymer electrolyte with 2 wt% of MnO_2 filler (C2Mn), which could be correlated to the increase in charge carriers or free ion percentage on dispersing the filler into the

polymer matrix [54]. With the help of the transference number (t_{ion}) obtained, the individual contribution of cations and anions in the transport parameters diffusion coefficient (D) and mobility (μ) can be substantiated using Eqs. 8, 9, 10 and 11,

$$D = D_+ + D_- = \frac{KT\sigma}{ne^2} \tag{8}$$

$$t_{ion} = \frac{D_-}{D_+ - D_-} = D_+/D \tag{9}$$

$$\mu = \mu_+ + \mu_- = \frac{\sigma}{nq} \tag{10}$$

$$t_{ion} = \frac{\mu_+}{\mu_+ + \mu_-} \tag{11}$$

$D+$, $D-$, μ_+ and μ_- denote the contribution of cations and anions in diffusion process (D) and mobility (μ), respectively [55]. It is obvious from Fig. 10 that the contribution of cations in both the diffusion coefficient and mobility is found to be higher in C2Mn than the polymer electrolyte without the filler CN60.

Stability window analysis

Figure 11 displays voltammograms of the electrolytes CN60 and C2Mn carried out against stainless steel (SS) electrodes using LSV analysis. LSV helps to validate the

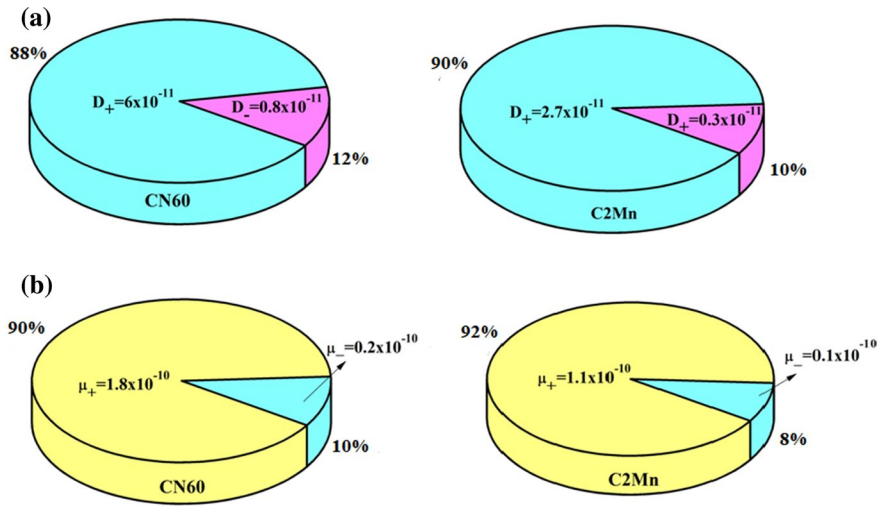

Fig. 10 Pie chart depicting the individual contribution of cations and anions in transport parameters **a** mobility(μ) and **b** diffusion coefficient (D) process in electrolytes CN60 and C2Mn

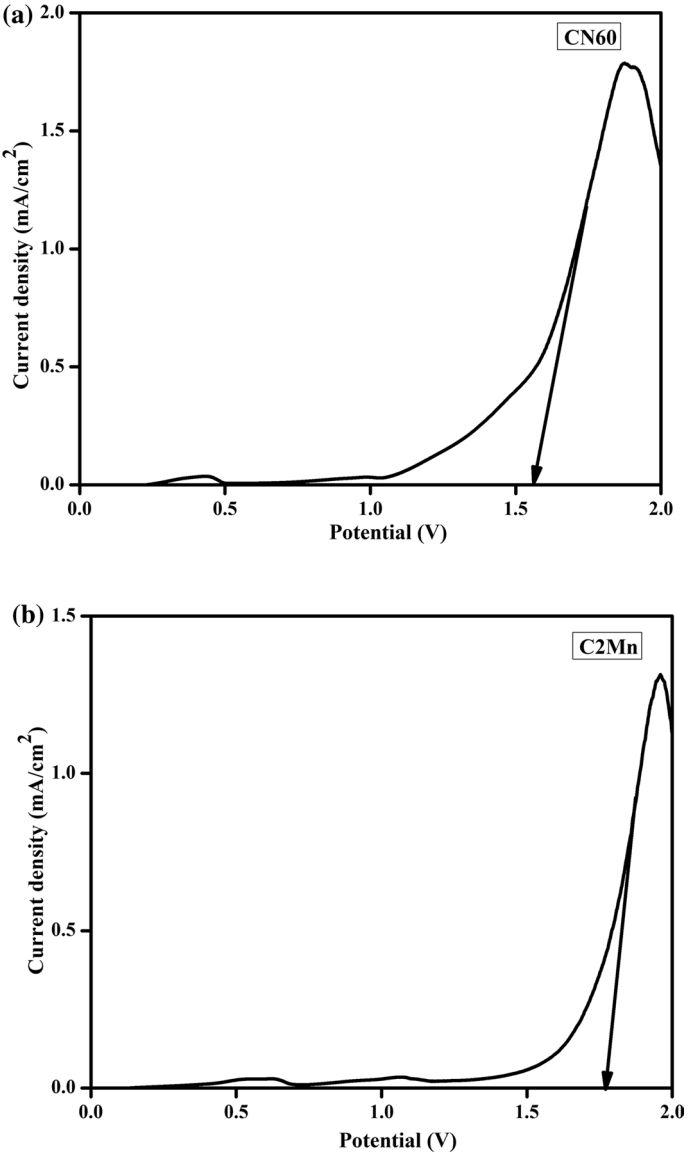

Fig. 11 LSV analysis of **a** CN60 and **b** C2Mn

improvement in the electrochemical voltage window of the highest salt-conducting polymer electrolyte (CN60) with the addition of 2wt% of MnO_2 (C2Mn). It is found that the stability window has been increased from 1.4 V to 1.7 V on adding MnO_2 filler. In addition, a prototype of primary magnesium battery with the highest conducting polymer electrolyte (C2Mn) has been fabricated and is given in Supplementary Information (Fig. S2) along with the observed open-circuit potential (OCP) and discharge profile

characteristics (Fig. S3). The OCP is the potential obtained when no external current is supplied between the anode and cathode terminals of the battery and the value is found to be around 1.7 V for 72 h. However, on discharging the battery through 100 kΩ sudden drop in the OCP value to 1.59 V has been observed along with discharge current of 89 µA for 72 h. The discharge capacity is around 6.5 mAh calculated using Eq. (12) [56]

$$\text{Discharge capacity} = \text{discharge current} \times \text{discharge time} \tag{12}$$

Conclusions

Thus, based on the obtained results, the significance of dispersing MnO_2 filler in increasing the ionic conductivity has been substantiated in the chitosan biopolymer electrolyte prepared with $MgNO_3.6H_2O$ salt. Consequently, the highest conductivity is achieved by one order of magnitude $(1.25 \pm 0.09) \times 10^{-3}$ Scm^{-1}) in the sample with 2 wt% of MnO_2. This is supported with the results obtained from XRD, DSC, TGA and FTIR analysis. The reduction in degree of crystallinity and glass transition temperature (T_g) values with the addition of MnO_2 filler, as evidenced by XRD and DSC results, indicates the creation of more free volume inside the polymer matrix along with an increase in number of charge carrier densities (n), ionic mobility (μ) and diffusion coefficient (D) values calculated from FTIR deconvolution analysis in absorption mode. These observations show that adding MnO_2 to the salt dissociated it into a significant number of free ions, inhibiting ion aggregation formation. The presence of ionic behaviour in the produced electrolytes has been further confirmed by the transference number analysis (t_{ion}). The electrochemical stability window extended to 1.7 V on the addition of MnO_2 filler in chitosan matrix, indicating the hopeful choice of the polymer electrolyte for device application.

Supplementary Information The online version contains supplementary material available at https://doi.org/10.1007/s00289-022-04411-y.

Author Contributions [PAH] performed conceptualization, methodology, formal analysis, investigation and writing—original draft preparation; [PCS] did supervision; [DL] and [MD] were involved in review and editing.

Funding The authors declare that no funds have been received during the preparation of manuscript.

Declarations

Conflict of interest The authors have not disclosed any conflicts.

References

1. Liu Y, Sun Z, Denis DK, Sun J, Liang L, Linrui H, Changzhou Y (2019) Recent progress in flexible non-lithium based rechargeable batteries. J Mater Chem A 7:4353–4382. https://doi.org/10.1039/C8TA10258A
2. Manthiram A, Yu X, Wang S (2017) Lithium battery chemistries enabled by solid-state electrolytes. Nat Rev Mater 2:16103. https://doi.org/10.1038/natrevmats.2016.103
3. Yang J, Zhang H, Zhou Q, Qu H, Dong T, Zhang M, Tang B, Zhang J, Cui G (2019) Safety-enhanced polymer electrolytes for sodium batteries: recent progress and perspectives. ACS Appl Mater Interfaces 11(19):17109–17127. https://doi.org/10.1021/acsami.9b01239
4. Asif M, Kilian S, Rashad M (2021) Uncovering electrochemistries of rechargeable magnesium-ion batteries at low and high temperatures. Energy Storage Mater 42:129–144. https://doi.org/10.1016/j.ensm.2021.07.031
5. Long MC, Wang T, Duan PH, Gao Y, Wang XL, Wu G, Wang YZ (2022) Thermotolerant and fireproof gel polymer electrolyte toward high-performance and safe lithium-ion battery. J Energy Chem 65:9–18. https://doi.org/10.1016/j.jechem.2021.05.027
6. Song S, Gao W, Yang G, Zhai Y, Yao J, Lin L, Tang W, Hu N, Lu L (2022) Hybrid poly-ether/carbonate ester electrolyte engineering enables high oxidative stability for quasi-solid –state lithium metal batteries. Mater Today Energy 23:100893. https://doi.org/10.1016/j.mtener.2021.100893
7. Yang G, Zhai Y, Yao J, Song S, Lin L, Tang W, Wen Z, Hu N, Lu L (2021) Chem. Synthesis and properties of poly(1,3-dioxalne) in situ quasi-solid state electrolytes via a rareearthtriflate catalyst. Commun 57:7934–7937. https://doi.org/10.1039/D1CC02916A
8. Chen P, Zheng Q, Li Q, Zhao R, Li Z, Wen X, Wen W, Liu Y, Chen A, Li Z, Liu X (2022) A ketone-containing all-solid state polymer electrolyte with rapid Li-ion conduction for lithium metal batteries. Chem Eng J 427:132025. https://doi.org/10.1016/j.cej.2021.132025
9. Liu Z, Wang X, Liu Z, Zhang S, Lv Z, Cui Y, Du L, Li K, Zhang G, Lin MC, Du H (2021) Low-Cost gel polymer electrolyte for high-performance aluminium-ion batteries. ACS Appl Mater Interfaces 13(24):28164–28170. https://doi.org/10.1021/acsami.1c05476
10. Gao L, Li J, Ju J, Cheng B, Kang W, Deng N (2020) Polyvinylidene fluoride nanofibers with embedded $Li_{6.4}La_3Zr_{1.4}Ta_{0.6}O_{1.2}$ fillers modified polymer electrolytes for high-capacity and long-life all-solid-state lithium metal batteries. Compos Sci Technol. 200:108408. https://doi.org/10.1016/j.compscitech.2020.108408
11. Gupta A, Jain A, Tripathi SK (2021) Strucutural, electrical and electrochemical studies of ionic liquid- based polymer gel electrolyte using magnesium salt for supercapacitor application. Polym Res 28:235. https://doi.org/10.1007/s10965-021-02597-9
12. Sravanthi K, Sundari GS, Erothu H (2021) Development of bio-degradable basaed polymer electrolytes for EDLC application. Optik 241:166229. https://doi.org/10.1016/j.ijleo.2020.166229
13. Patel S, Kumar R (2021) Effect of Al_2O_3 on electrical properties of polymer electrolyte for electrochemical device application. Mater Today: Proc 46:2175–2178. https://doi.org/10.1016/j.matpr.2021.02.691
14. Ponraj T, Ramalingam A, Selvasekarapandian S, Srikumar SR, Manjuladevi R (2021) Plasticized solid polymer electrolyte based on triblock copolymer poly(vinylidene chloride-co-acrylonitrile-co-methyl methacrylate) for magnesium ion batteries. Polym Bull 78:35–57. https://doi.org/10.1007/s00289-019-03091-5
15. Cheng J, Hou G, Chen Q, Li D, Li K, Yuan Q, Wang J, Ci L (2022) Sheet-like garnet structure design for upgrading PEO-based electrolyte. Chem Eng J 429:132343. https://doi.org/10.1016/j.cej.2021.132343
16. Cui P, Zhang Q, Sun C, Gu J, Shu M, Gu J, Shu M, Gao C, Zhang Q, Wei W (2022) High ion conductivity based on a polyurethane composite solid electrolyte for all-solid-state lithium batteries. RSC Adv 12:3828–3837. https://doi.org/10.1039/D1RA07971A
17. Mathew DE, Gopi S, Kathiresan M, Stephan AM, Thomas S (2019) Influence of MOF ligands on the electrochemical and interfacial properties of PEO-based electrolytes for all-solid-state lithium batteries. Electrochim Acta 319:189–200. https://doi.org/10.1016/j.electacta.2019.06.157
18. Zang G, He M, Liao Y, Li M, Hong M, Li W (2022) Electrochemical improvement in high-voltage Li-ion batteries by electrospinning a small amount of nano-Al_2O_3 in P(MVE-MA)/P(VdF-HFP)-blended gel electrolyte. Ionics 28:767–777. https://doi.org/10.1007/s11581-021-04351-z

19. Rayung M, Aung MM, Azhar SC, Adsullah LC, Su'ait MS, Ahmad A, Jaamil SN, (2020) Bio-based polymer electrolytes for electrochemical devices: insight into the ionic conductivity performance. Materials 13(4):838. https://doi.org/10.3390/ma13040838
20. Roy BK, Tahmid I, Rashid TU (2021) Chitosan-based materials for supercapacitor applications: a review. J Mater Chem A 9:17592–17642. https://doi.org/10.1039/D1TA02997E
21. Panda PK, Dash P, Yang JM, Chang YH (2022) Development of chitosan, graphene oxide, and cerium oxide composite blended films: structural, physical, and functional properties. Cellulose 29:2399–2411. https://doi.org/10.1007/s10570-021-04348-x
22. Alves R, Sabadini RC, Gonçalves TS, De Camargo ASS, Pawlicka A, Silva MM (2019) Structural, morphological, thermal and electrochemical characteristics of chitosan: praseodymium triflate based solid polymer electrolytes. Int J Green Energy 16(15):1602–1610. https://doi.org/10.1080/15435075.2019.1677239
23. Sun W, Chen L, Wang Y, Zhou Y, Meng S, Li H, Luo Y (2016) Synthesis of highly conductive PPy/Graphene/MnO_2 Composite using ultrasonic irradiation. Synth React Inorg Met-Org Chem 46(3):437. https://doi.org/10.1080/15533174.2014.98825
24. Johan MR, Ting LM (2011) Strucutal, thermal and electrical properties of nano manganese-composite polymer electrolytes. Int J Electrochem Sci 6:4737
25. Li Y, Sun Z, Liu D, Gao Y, Wang Y, Bu H, Li M, Zhang Y, Gao G, Ding S (2020) A composite solid polymer electrolyte incorporating MnO_2 nanosheets with reinforced mechanical properties and electrochemical stability for lithium metal batteries. J Mater Chem A. https://doi.org/10.1039/C9TA11542K
26. Tan SM, Johan MR (2011) Effects of MnO_2 nano-particels on the conductivity of PMMA-PEO-$LiClO_2$-EC polymer electrolytes. Ionics 17:485. https://doi.org/10.1007/s11581-011-0541-7
27. Sulaiman M, Rahman A, Mohamed NS (2013) Strucural, thermal and conductivity studies of Magnesium Nitrate-Alumina Composite Solid electrolytes prepared via Sol-gel method. Int J Electrochm Sci 8:6647
28. Khan NM, Mazuki NF, Samsudin AS (2022) Contribution of Li+ ions to a gel polymer electrolyte based on polymethyl methacrylate and polylactic acid doped with lithium bis (oxalate) borate. J Electron Mater 51:745. https://doi.org/10.1007/s11664-021-09372-y
29. Poosapati A, Negrete K, Thorpe M, Hutchison J, Zupan M, Lan Y, Madan D (2021) Safe and flexible chitosan-based polymer gel as an electrolyte for use in zinc-alkaline based chemistries. J Appl Polym Sci 138(33):50813. https://doi.org/10.1002/app.50813
30. Rahman NA, Navaratnam S, Abidin SZ, Latif FA (2018) FTIR study on the effect of free ions in PMMA/ENR 50 polymer electrolyte system 2020 AIP Conf. Proc 1:020076. https://doi.org/10.1063/1.5062702
31. Majumdar S, Sen P, Ray R (2019) Ionic interactions and transport properties in chitosan-starch based blend solid biopolymer electrolytes. Mater Today: Proc. 18:4913–4920. https://doi.org/10.1016/j.matpr.2019.07.483
32. Mylarappa M, Lakshmi VV, Mahesh KV, Nagaswarupa HP, Raghavendra N (2016) A faciel hydrothermal recovery of nano sealed MnO_2 particel from waste batteries: an advanced material for electrochemical and environmrntal applications. IOP Conf Ser: Mater Sci Eng. https://doi.org/10.1088/1757-899X/149/1/012178
33. Nancy AC, Suthanthiraraj SA (2017) Effect of Al_2O_3 nanofiller on the electrical, thermal and structural properties of PEO: PPG based nanocomposite polymer electrolyte. Ionics 23:1439. https://doi.org/10.1007/s11581-017-1976-2
34. Shamsuri NA, Zaine SN, Yusof YM, Yahya WZ, Shukur MF (2020) Effect of ammonium thiocyanate on ionic conductivity and thermal properties of polyvinyl alcohol-methylcellulose- based polymer electrolytes. Ionics 26:6083. https://doi.org/10.1007/s11581-020-03753-9
35. Sundararajan V, Saidi NM, Ramesh S, Ramesh K, Selvaraj G, Wilfred CD (2019) Quasi solid-state dye-sensitized solar cell with P(MMA-co-MAA) based polymer electrolytes. J Solid State Electrochem 23:1179. https://doi.org/10.1007/s10008-019-04207-7
36. Arya A, Sharma AL (2018) Effect of salt concentration on dielectric properties of Li-ion conducting blend polymer electrolytes. J Mater Sci: Mater Electron 29:17903–17920. https://doi.org/10.1007/s10854-018-9905-3
37. Rahman NA, Hanifah SA, Mobarak NN, Ahmad A, Ludin NA, Bella F, Su'ait MS (2021) Chitosan as a paradigm for biopolymer electrolytes in solid-state dye-sensitised solar cells. Polymer 230:124092. https://doi.org/10.1016/j.polymer.2021.124092

38. Chowdhury FI, Islam J, Arof AK, Khandaker MU, Zabed HM, Khalil I, Rahman MR, Islam SM, Karim MR, Uddin J (2021) Electrocatalytic and structural properties and computational calculation of PAN-EC-PC-TPAI-I_2 gel polymer electrolytes for dye sensitized solar cell application-**RSC**. Adv 11:22937–22950. https://doi.org/10.1039/D1RA01983J
39. He R, Kyu T (2016) Effect of plasticization on ionic conductivity enhancement in relation to glass transition temperature of crosslinked polymer electrolyte membranes. Macromolecules 49(15):5637–5648. https://doi.org/10.1021/acs.macromol.6b00918
40. Bocharova V, Sokolov AP (2020) Perspectives for polymer electrolytes: A view from fundamentals of ionic conductivity. Macromolecules 53(11):4141. https://doi.org/10.1021/acs.macromol.9b02742
41. Money BK, Hariharan K, Swenson J (2012) Glass Transition and relaxation processes of nanocomposite polymer electrolytes. J Phys Chem B 116(26):7762. https://doi.org/10.1021/jp3036499
42. Hu J, Wang W, Yu R, Guo M, He C, Xie X, Peng H, Xue Z (2017) Solid polymer electrolyte based on ionic bond or covalent bond functionalized silica nanoparticels. RSC Adv 7:54986–54994. https://doi.org/10.1039/C7RA08471D
43. Dueramae I, Okhawilai M, Kasemsiri P, Uyama H (2021) High electrochemical and mechanical performance of zinc conducting based gel polymer electrolytes. Sci Rep 11:13268. https://doi.org/10.1038/s41598-021-92671-5
44. Koduru HK, Marinov YG, Kaleemulla S, Rafailov PM, Hadjichristov GB, Scaramuzza N (2021) Fabrication and characterization of magnesium-ion conducting flexible polymer electrolyte membranes based on a nanocomposite of poly (ethylene oxide) and potato starch nanocrystals. J Solid State Electrochem 25:2409. https://doi.org/10.1007/s10008-021-05018-5
45. Ganta KK, Jeedi VR, Katrapally VK, Yalla M, Emmadi LN (2021) Effect of TiO_2 nano-filler on electrical properties of Na^+ ion conducting PEO/PVDF based blended polymer electrolyte. J Inorg Organomet Polym 31:3430. https://doi.org/10.1007/s10904-021-01947-w
46. Xu L, Li J, Deng W, Li L, Zou G, Hou H, Huang L, Ji X (2021) Boosting the ionic conductivity of PEO electrolytes by waste eggshell-derived fillers for high-performance solid lithium/sodium batteries. Mater Chem Front 5:1315. https://doi.org/10.1039/D0QM00541J
47. Kamboj V, Arya A, Tanwar S, Kumar V, Sharma AL (2021) Nanofiller assisted Na^+ conducting polymer nanocomposite for ultracapacitor: structural, dielectric and electrochemical properties. Mater Sci 56:6167. https://doi.org/10.1007/s10853-020-05667-3
48. Salehan SS, Nadirah BN, Saheed MS, Yahya WZ, Shukur MF (2021) Conductivity, structural and thermal properties of corn starch-lithium iodide nanocomposite polymer electrolyte incorporated with Al_2O_3. J Polym Res 28:222. https://doi.org/10.1007/s10965-021-02586-y
49. Majumdar S, Sen P, Ray RJ (2022) High performace graphene oxide-grafted chitosan-starch solid biopolymer electrolytes for flexible hybrid supercapacitors Solid. State Electrochem 26:527. https://doi.org/10.1007/s10008-021-05093-8
50. Majumdar S, Sen P, Ray RJ (2022) CNT assisted anomalous Li^+ transport in CS/CMC solid biopolymer nanocomposite: an electrolyte in hybrid solid-state supercapacitors. Ionics 28:1403. https://doi.org/10.1007/s11581-021-04389-z
51. Sudaryanto,Yulianti E, Patimatuzzohrah, (2016) Strucure and properties of solid polymer electrolyte based on chitosan and ZrO_2 nanoparticle for Lithium ion battery. In: AIP. Conference Proceedings 1710 (1), 020003. https://doi.org/10.1063/1.4941464
52. Helen PA, Ajith K, Diana MI, Lakshmi D, Selvin PC (2022) Chitosan based biopolymer electrolyte reinforced with V_2O_5 filler for magnesium batteries : an inclusive investigation. J Mater Sci- Mater Electron 33:3925. https://doi.org/10.1007/s10854-021-07587-7
53. Jenova I, Venkatesh K, Karthikeyan S, Madeswaran S, Aristatil G, Moni P, Sheeba DJ (2021) Solid polymer electrolyte based on tragacanth gum-ammonium thiocyanate. J Solid State Electrochem 25:2371. https://doi.org/10.1007/s10008-021-05016-7
54. Choi BN, Yang JH, Kim YS, Chung CH (2019) Effect of morphological change of copper-oxide fillers on the performance of solid polymer electrolytes for lithium-metal polymer batteries. RSC Adv 9(38):21760–21770. https://doi.org/10.1039/C9RA03555A
55. Ramli MA, Isa MIN (2016) Structural and ionic transport properties of protonic conducting solid biopolymer electrolytes based on carboxymethyl cellulose doped with ammonium fluoride. J Phys Chem B 120(44):11567–11573. https://doi.org/10.1021/acs.jpcb.6b06068

56. Rani MSA, Mohammad M, Suait MS, Ahmad A, Mohamed NS (2021) Novel approach for the utilization of ionic liquid-based cellulose derivative biosourced polymer electrolytes in safe sodium-ion batteries. Polym Bull 78:5355–5377. https://doi.org/10.1007/s00289-020-03382-2

Authors and Affiliations

P. Adlin Helen[1] · P. Christopher Selvin[1] · D. Lakshmi[2] · M. Infanta Diana[1]

[1] Luminescence and Solid State Ionics Laboratory, Department of Physics, Bharathiar University, Coimbatore, Tamil Nadu 641046, India

[2] Department of Physics, PSG College of Arts and Science, Coimbatore, Tamil Nadu 641014, India